Optimal Number of Angle Images for Calculating Anterior Angle Volume and Iris Volume Measurements

Lauren S. Blieden,[1,2] Alice Z. Chuang,[1] Laura A. Baker,[2] Nicholas P. Bell,[1,2] Timothy S. Fuller,[1,2] Kimberly A. Mankiewicz,[1] and Robert M. Feldman[1,2]

[1]Ruiz Department of Ophthalmology and Visual Science, The University of Texas Medical School at Houston, Houston, Texas, United States
[2]Robert Cizik Eye Clinic, Houston, Texas, United States

Correspondence: Lauren S. Blieden, 6400 Fannin Street, Suite 1800, Houston, TX 77030, USA lblieden@cizikeye.org.

Submitted: October 15, 2014
Accepted: March 17, 2015

Citation: Blieden LS, Chuang AZ, Baker LA, et al. Optimal number of angle images for calculating anterior angle volume and iris volume measurements. *Invest Ophthalmol Vis Sci*. 2015;56:2842–2847. DOI:10.1167/iovs.14-15883

Purpose. We determined the optimal number of angle images required to obtain reliable measurements of trabecular-iris circumferential volume (TICV) and iris volume (IV) using swept-source Fourier domain anterior segment optical coherence tomography (SSFD-ASOCT) scans in narrow angle eyes.

Methods. Scleral spur landmarks (SSL) were manually identified on ASOCT angle images from 128 meridians from each of 24 eyes with chronic primary angle closure (PAC) spectrum of disease. The anterior and posterior corneal curves, and the anterior and posterior iris surfaces were identified automatically by the anterior chamber analysis and interpretation (ACAI) software, then manually examined and edited by the reader if required. Trabecular-iris circumferential volume at 750 μm from SSL (TICV750) and IV were subsequently calculated using varying numbers of angle images. Threshold error was determined to be less than the lower 95% confidence limit of mean absolute percent error (MAPE) of the change in TICV or IV resulting from laser peripheral iridotomy, which would be 17% for TICV and 5% for IV, based on previous studies. The optimal number of angle images was the smallest number of images where MAPE was less than this threshold for TICV and IV.

Results. A total of 32 equally-spaced angle images (16 meridians) was required to estimate TICV750 and 16 angle images (8 meridians) to estimate IV. Both were within 4.6% and 1.6% of MAPE, respectively.

Conclusions. It is possible to determine TICV and IV parameters reliably in narrow angles without evaluating all 128 meridians obtained with SSFD-ASOCT.

Keywords: anterior segment optical coherence tomography, iris volume, angle, trabecular-iris circumference volume

Changes in peripheral angle configuration and iris volume (IV) have an important role in the pathogenesis of the primary angle closure (PAC) spectrum of disease.[1,2] Monitoring changes in angle configuration over time, evaluating effect of narrow angle treatment, such as laser peripheral iridotomy (LPI) or lens extraction (LE), and studying changes in IV from light to dark depend on the accuracy and precision of angle and iris measurements. Currently, the accepted gold standard for viewing the anterior chamber angle is gonioscopy. While gonioscopy is an invaluable part of the clinical exam in PAC spectrum patients, it is a subjective and sometimes difficult technique, even in the hands of experienced ophthalmologists. In addition, Quigley et al.[1] and Aptel et al.[3] proposed that small iris cross-sectional area changes or small IV changes with physiologic pupil dilation are potential risk factors for PAC. These small changes in either cross-sectional area or volume of the iris can be evaluated only by imaging techniques, such as anterior segment optical coherence tomography (ASOCT) or ultrasound biomicroscopy (UBM).

Several ASOCT devices have been developed in the last decade.[4] These devices can produce reliable cross-sectional measurements of the angle.[5–8] However, because of slow scan speeds, only two meridians (horizontal and vertical), or four angle measurements, can be feasibly acquired in each sitting. While this provides a snapshot view of the angle anatomy, it cannot produce a circumferential view of the peripheral angle and iris. Improvements in imaging technology with newer generation ASOCT instruments, such as the CASIA SS-1000 (Tomey Corporation, Nagoya, Japan), have substantially improved imaging capability and speed, allowing imaging of 128 meridians (256 angle images) in approximately 2.4 seconds, thereby providing more information about the circumference of the angle and iris.[4–10] Because the angle landmarks still must be identified manually, with this many scans to analyze, the process for quantifying peripheral angle anatomy becomes very labor-intensive and time-consuming. Objective anterior chamber volume measurements are important to monitor small changes in the peripheral angle, which may result in angle closure.[11]

The purpose of this study was to determine the minimum number of angle images taken at equally spaced meridians required to estimate trabecular-iris circumferential volume (TICV) and IV in narrow angle eyes with minimal acceptable measurement error.

Methods

This retrospective study was conducted at the Robert Cizik Eye Clinic of the Ruiz Department of Ophthalmology and Visual

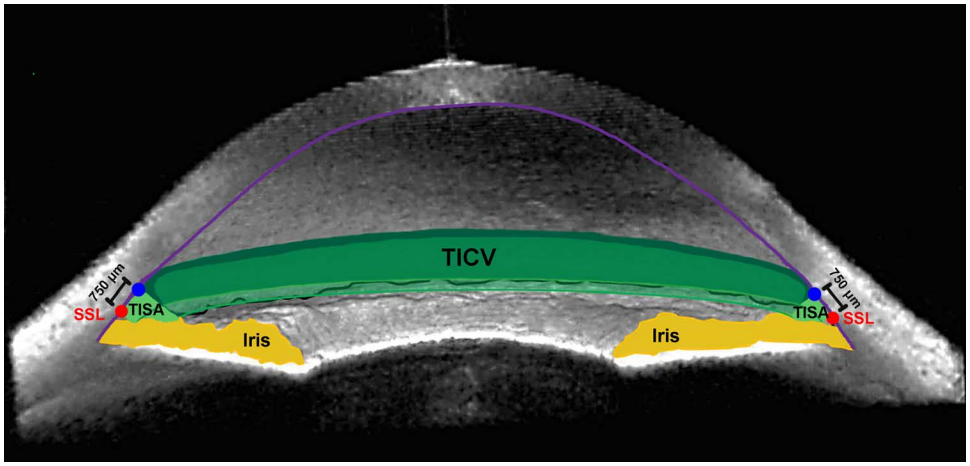

FIGURE 1. Trabecular-iris circumferential volume. A 3D ASOCT angle image exhibiting TISA750 (*light green space*) and TICV750 (*darker green spaces*), along with the SSL (*red circle*), iris (*yellow*), and cornea (*violet line*). Adapted from Rigi M, Blieden LS, Nguyen D, et al. Trabecular-iris circumference volume in open angle eyes using swept-source Fourier domain anterior segment optical coherence tomography. *J Ophthalmol*. 2014;2014:590978.[11]

Science at The University of Texas Medical School at Houston (Houston, TX, USA). The Committee for the Protection of Human Subjects at The University of Texas Health Science Center determined that this study was exempt from review. All research adhered to the tenets of the Declaration of Helsinki and was Health Insurance Portability and Accountability Act (HIPAA) compliant.

Participants

Patients with eyes classified as PAC spectrum[12] who underwent ASOCT imaging between September 2011 and July 2012 were identified during a chart review. Participants with PAC spectrum disease (defined by gonioscopy as the deepest possible structure visible without compression being the anterior TM [Spaeth grade A or B],[13,14] or with evidence of plateau iris) were included. Eyes must have been imaged using a standard imaging protocol in a dark room with no external light by the CASIA SS-1000 using the 3D mode with angle analysis scan.[11,15] Eyes were excluded if they had prior intraocular incisional surgery, intraocular injections, or extraocular surgery, or if they had any anterior segment abnormalities that affected the angle or measurements (i.e., significant corneal opacity). In addition, eyes were excluded if the image quality was not acceptable (i.e., blink or eyelid obstruction). If both eyes were eligible, one eye was randomly selected by coin toss (heads = right and tails = left).

Image Reading

The scans were exported raw from the CASIA SS-1000 and read by an experienced reader (AZC), who was masked to gonioscopy grade, using customized software, Anterior Chamber Angle and Interpretation (ACAI, Houston, TX, USA) as described previously.[11,15] After identifying the scleral spur landmarks (SSLs), examining and adjusting all 128 meridian images, the interpretation result was saved, the refraction correction processed, and angle parameters, including angle opening distance at 750 µm (AOD750),[11,15,16] trabecular-iris space area at 750 µm (TISA750),[11,15,17] iris cross-sectional area (ICSA), and radius of TISA750 (R_{TISA}),[11] as well as radius of ICSA (R_{ICSA})[3] were calculated and saved for each angle.

TICV and IV

Trabecular-iris circumferential volume is the integrated volume of the peripheral angle taken from TISA measurements as described previously (Fig. 1).[11] Iris cross-sectional area is the area bordered by the anterior iris surface, anterior surface of the demarcation line created by the reflection of the posterior layer of pigment epithelium, and line drawn from SSL and parallel to the visual axis (Fig. 2A). Iris volume is the integrated iris cross-sectional area measured around the angle (Fig. 2B).

Trabecular-iris circumferential volume at 750 (TICV750)[11] and IV were calculated based on Pappus's centroid theorem. R_{TISA} or R_{ICSA} is the distance from the centroid of TISA or ICSA to the midpoint of the scleral spur landmark-to-landmark line (Fig. 2A). The values of $TICV750_n$ and IV_n are the volumes calculated using n equally spaced angle images, $n = 2$ (temporal and nasal), 4, 16, 32, 64, 128, and 256. The formulas for $TICV750_n$ and IV_n are

$$TICV750_n = 2\pi \sum_{i=1}^{n} TISA750_i R_{TISA_i}/n \quad \text{and}$$

$$IV_n = 2\pi \sum_{i=1}^{n} ICSA_i R_{ICSA_i}/n,$$

respectively.

Evaluating Measurement Error

As every border for calculating TISA750 was examined manually, using all 256 TISA750s to calculate $TICV750_{256}$ should be the most accurate measurement for each eye. The TICV750 measurement error from n angle images (<256) was defined as ($TICV750_n - TICV750_{256}$), absolute error as ($|TICV750_n - TICV750_{256}|$), and absolute percent error as ([$|TICV750_n - TICV750_{256}|$) / $TICV750_{256}$]*100%) for each eye. Error, absolute error, and absolute percent error for IV were calculated in the same fashion.

Determining Acceptable TICV Measurement Error

The threshold error should be less than the lower 95% confidence limit of the change in TICV resulting from LPI, since this is what we wish to measure. From our data (Nguyen D, et al. *IOVS* 2013;54:ARVO E-Abstract 4812), Memarzadeh et al.,[18] and Lee et al.,[19] the estimated lower 95% confidence limit for the LPI effect on TISA750 is approximately 17% change from before LPI. The effect of LPI on TICV is not yet known.

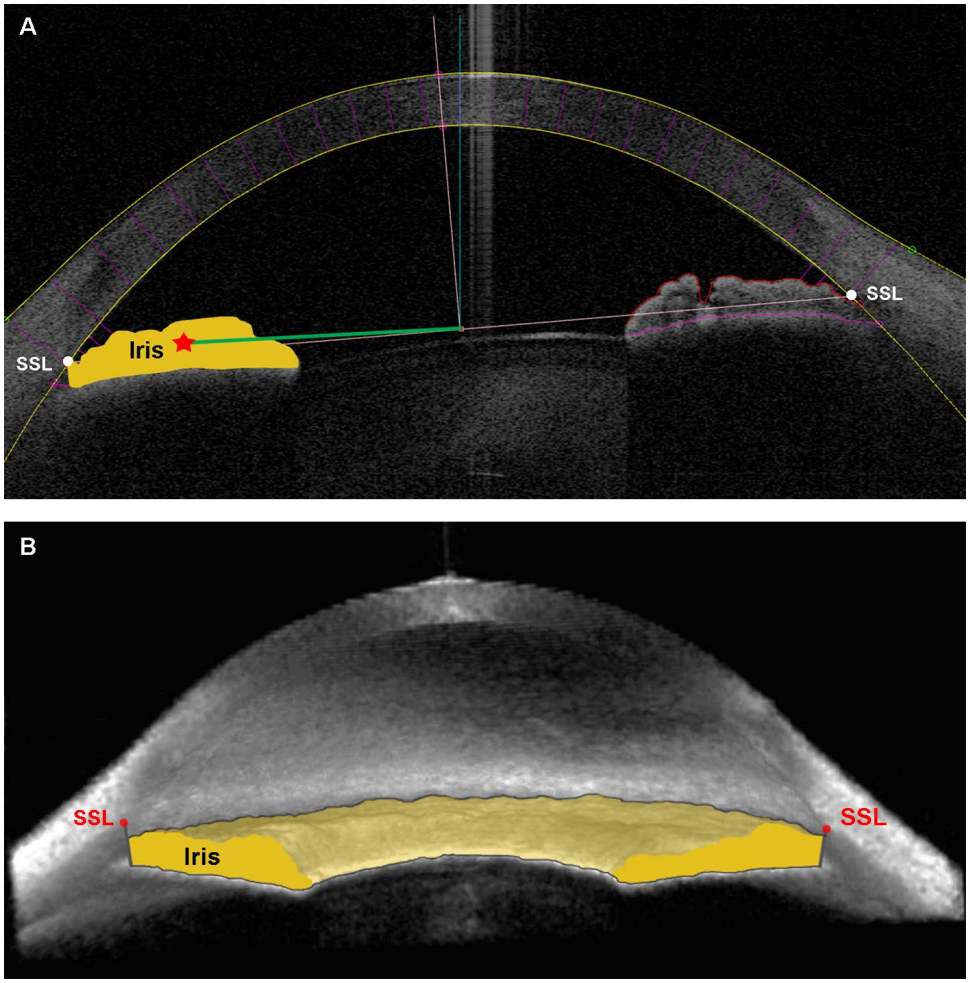

FIGURE 2. Iris volume. (**A**) The 2D and (**B**) 3D ASOCT angle images exhibiting borders for IV calculation. Iris cross-sectional area is the area bordered by anterior iris surface, anterior surface of the demarcation line created by the reflection of the posterior layer of pigment epithelium, and the line drawn from SSL and parallel to visual axis. R_{ICSA} is represented by the *green line*. (**A**). Iris volume is the integrated iris cross-sectional area measured around the angle (**B**). The SSL appears above the iris plane in the 3D view of this open-angle eye.[15]

However, the effect should be similar to TISA (as TICV is derived from TISA), and it is reasonable to extrapolate the results from TISA to TICV. Therefore, the optimal number of angle images for TICV750 was determined to be the smallest number of angles (n) for which the upper 95% confidence limit of mean absolute percent error (MAPE) was less than 17%.

Determining Acceptable IV Measurement Error

Aptel et al.[20] found that the post-LPI mean IV increased 7% from baseline in pigment dispersion syndrome eyes with pharmacologic mydriasis. The SD of change was not reported; however, the SDs of the changes between 3 paired dilation conditions were all less than 0.3 µL (or 0.7%).[20] Taking a conservative approach, the SD of IV change due to LPI was estimated to be 1%. The lower 95% confidence limit for IV change was approximately 5%. Therefore, the optimal number of angle images for IV was determined by the smallest number of angle images (n) for which the upper 95% confidence limit of MAPE was less than 5%.

Data Analysis

Demographics were summarized by mean and SD for continuous variables or by frequency (%) for discrete variables. Means of $TICV750_n$, IV_n, error, absolute error, absolute percent error, and their corresponding SDs and 95% confidence limits were computed for each n. All analyses were performed using SAS software version 9.3 for Windows (SAS Institute, Inc., Cary, NC, USA).

RESULTS

We included 24 eyes. Four (17%) of the participants were male. There were 11 white (46%), 7 black (29%), 5 Hispanic (21%), and 1 Asian (4%) participants. The mean age was 57.7 years (±10.3). Of the eyes 50% ($N = 12$) had only Schwalbe's line visible on gonioscopy grading, and one eye had plateau iris syndrome with posterior trabecular meshwork visible on gonioscopy. A total of 12 eyes (50%) had peripheral anterior synechiae (PAS), with one eye not able to be examined gonioscopically. There were 17 eyes (71%) with cataracts, and 4 (16%) eyes were on IOP-lowering medications (Table 1).

Table 2 shows the means (±SD) of TICV750, error, absolute error, and absolute percent error for each number of angle images. Mean TICV750 was 1.969 (±1.012) µL using all 256 angle images and 2.584 (±1.367) µL using only the horizontal meridian (two angle images). The mean absolute error (MAE) was reduced from 0.644 (±0.599) µL using two horizontal

Table 1. Demographics and Ocular Characteristics

Variable	Statistics, $N = 24$
Age, mean y ± SD (min to max)	57.67 ± 10.33 (45–76)
Sex, *N* male (%)	4 (17%)
Race, *N* (%)	
White	11 (46%)
Black	7 (29%)
Hispanic	5 (21%)
Asian	1 (4%)
Study eye, *N* right (%)	12 (50%)
Gonioscopy, *N* (%)	
Schwalbe's line visible	12 (50%)
Anterior TM visible	11 (46%)
Posterior TM visible	1 (4%)
PAS present, *N* (%)*	12 (52%)
Cataract present, *N* (%)	17 (71%)
IOP, mean mm Hg ± SD (min to max)	16.04 ± 3.69 (9–25)
Number of IOP-lowering medications, *N* (%)	
0	20 (83%)
1	2 (8%)
2	1 (4%)
3	1 (4%)

PAS, peripheral anterior synechiae; TM, trabecular meshwork.
* One data point missing.

meridian angle images to 0.275 (±0.223) μL using horizontal and vertical meridians (four angle images). However, the MAPE for both meridians was 18.2% (±21.4%). The MAPE was reduced to 4.6% (±4.0%), with upper 95% confidence limit of 12.4%, at 32 angle images (16 meridians), which met the predetermined threshold of the upper 95% confidence limit of MAPE equaling less than 17%.

Table 3 shows the means (±SD) of IV, error, absolute error, and absolute percent error for each number of angle images. Mean IV was 38.34 (±4.64) μL using all 256 angle images, while, unlike TICV750, mean IV was smaller (35.86 ± 4.76 μL) when it was estimated using only the horizontal meridian. The MAE was reduced from 2.54 (±1.70) μL using two horizontal meridian angle images to 0.96 (±0.74) μL using horizontal and vertical meridians (four angle images). However, the MAPE for both meridians was 2.5% (±1.8%) and, therefore, did not meet the predetermined threshold. The MAPE was reduced to 1.6% (±1.3%), with the upper 95% confidence limit of 4.1% at 16 angle images (8 meridians), which met the pre-determined threshold of the upper 95% confidence limit of MAPE less than 5%.

Discussion

In this study, we optimized the number of angle images required for reliable measurements of TICV and IV in narrow angle eyes while minimizing acceptable error. Our ultimate goal is that TICV will be used as a clinical parameter for evaluating treatment effect in narrow angle patients. In a previous study,[21] TICV was computed in pre- and post-LPI patients using all 128 meridians to objectively quantify the change in angle volume due to the effect of LPI. As this is an extremely time-consuming task, we decided to investigate whether we could achieve reasonably accurate results analyzing fewer images, thereby making the calculation of TICV more efficient without sacrificing the accuracy of the result. Our results indicated that to reach an acceptable minimum error in calculation, a minimum of 32 angle images (16 meridians) are required to calculate TICV750 and 16 angle images (8 meridians) are required to calculate IV.

We chose PAC patients, including those with PAS, as our population for this study. We previously demonstrated that the SD of TISA increased as TISA increases.[15] However, there is more variability in the angle in narrow angle eyes with PAS than those without PAS, because some portions will be closed with PAS, and some portions likely will be open. Since the patient population and disease process on which this measurement would be of potential value is narrow angles, using normal subjects may overestimate the measurement error and require more images to be read than actually are needed in the target population. The more variability, the more images (a conservative method) that would be required to predict 360° measurements, making this a more useful measurement. Excluding eyes with PAS, the very population where this measurement is potentially useful, would gear us to falsely low number of images required.

Previously, peripheral angle volume was estimated using anterior chamber depth (ACD). While the correlation between ACD and peripheral angle volume has not been investigated to our knowledge, using ACD as a substitute for peripheral angle volume probably is not as accurate in detecting the small changes important clinically in peripheral angle volume. The ability of TICV to measure peripheral angle volume directly makes it a potentially valuable tool for evaluating glaucoma. However, even though an age-adjusted normal reference range has been established for TICV,[11] until now, there are no studies to our knowledge evaluating TICV in the setting of anterior segment abnormality, pseudophakia, or PAC. This study paves the way for future investigations by improving the efficiency in evaluating this potentially useful parameter.

Previous studies have quantified IV.[3,20,22–24] While several of these studies had similar IVs to those in our study, it is difficult to compare their results because of varying study populations, analysis methods, and software. Also, these studies only used the Visante ASOCT (Carl Zeiss Meditec, Inc., Dublin, CA, USA), which is, at most, capable of measuring eight angle images (four meridians), limiting the extrapolation of IV across the entire iris. As we found, to minimize acceptable error, at least 16 angle images (8 meridians) are required. Finally, it is not clear where the iris measurement borders were defined.

Table 2. Estimates and Errors: TICV750 (μL) From SSLs

Number of Angle Images	TICV750 ± SD, μL	Error ± SD, μL	MAE ± SD, μL	MAPE ± SD, %
2, 180°; N/T	2.5836 ± 1.3665	0.6145 ± 0.6305	0.6439 ± 0.5990	36.2 ± 28.7
4, 90°; N/S/T/I	2.0286 ± 1.0261	0.0595 ± 0.3537	0.2752 ± 0.2231	18.2 ± 21.4
8, 45°	1.9994 ± 1.0324	0.0302 ± 0.2179	0.1719 ± 0.1327	11.2 ± 11.3
16, 22.5°	1.9910 ± 0.9945	0.0218 ± 0.1470	0.1105 ± 0.0968	7.4 ± 8.7
32, 11.25°	1.9834 ± 1.0169	0.0142 ± 0.0906	0.0736 ± 0.0526	4.6 ± 4.0
64, 5.63°	1.9752 ± 1.0070	0.0060 ± 0.0156	0.0132 ± 0.0099	0.9 ± 0.9
128, 2.81°	1.9730 ± 1.0108	0.0012 ± 0.0058	0.0040 ± 0.0042	0.3 ± 0.5
256, 1.41°	1.9692 ± 1.0122	0	0	0

N, nasal; T, temporal; S, superior; I, inferior.

Table 3. Estimates and Errors: IV (μL)

Number of Angle Images	Iris Volume ± SD, μL	Bias ± SD, μL	MAE ± SD, μL	MAPE ± SD, %
2, 180°; N/T	35.86 ± 4.76	−2.28 ± 1.79	2.54 ± 1.70	6.6 ± 4.0
4, 90°, N/S/T/I	37.80 ± 4.68	−0.54 ± 1.10	0.96 ± 0.74	2.5 ± 1.8
8, 45°	38.07 ± 4.58	−0.27 ± 0.80	0.63 ± 0.55	1.6 ± 1.3
16, 22.5°	38.29 ± 4.65	−0.05 ± 0.52	0.37 ± 0.36	0.9 ± 0.9
32, 11.25°	38.25 ± 4.55	−0.09 ± 0.23	0.19 ± 0.16	0.5 ± 0.4
64, 5.63°	38.32 ± 4.65	−0.01 ± 0.09	0.06 ± 0.07	0.1 ± 0.2
128, 2.81°	38.33 ± 4.64	−0.01 ± 0.04	0.03 ± 0.03	0.1 ± 0.1
256, 1.41°	38.34 ± 4.64	0	0	0

Particularly, the peripheral border of iris may have been demarcated differently in the other studies.

Tun et al.[25] and Mak et al.[26] also used the CASIA SS-1000 to measure IV in Chinese angle closure eyes. The value reported by Tun et al.[25] of 34.57 μL for closed angles is smaller than our estimate, while the value reported by Mak et al.[26] of 38.8 μL is essentially the same as ours. The disparity in values between the two studies may be due to the analysis method using the pixels on the 3D image produced by the CASIA SS-1000.[25,26] Our analysis method involves determining SSLs. Mak et al.[26] and Tun et al.[25] appear to use the 3D image to determine the iris root in their calculations, which can be harder to identify than the SSL, particularly on the closed angle images.

The same limitations described above and previously for calculating peripheral angle volume over the entire angle[11] apply to calculating total IV, especially in eyes that have already had an LPI. One unique limitation of calculating IV using ASOCT is that the posterior surface of the iris often is not directly visible for two reasons: (1) pigmentation limits the transmission of light and (2) the frequencies used for ASOCT have a limited depth of penetration.[27] However, based on histologic features of normal iris, this difference should be minimal and uniform as the posterior surface of the iris tends to be relatively flat, with more significant variability occurring on the anterior iris surface.[28]

The limitations of our study included the inherent limitations of a retrospective study. Some manual adjustments to measurements were made, which limits automatic and objective interpretation of results. Because participants were drawn from a pool of PAC spectrum patients, even though the reader of our images was masked to the gonioscopic grade, there may be bias resulting from knowledge that the pool of participants all had narrow angles. This potentially may have biased the ultimate calculation of TICV750 toward smaller measurements; however, this should not affect the results of the study in terms of the optimization of the number of angle images that must be read.

Our study demonstrated that further research into ASOCT imaging would be beneficial given the important clinical data about the angle that can be obtained rapidly and efficiently to better diagnose and treat angle closure–related disease entities.

Acknowledgments

Previously presented at the 24th American Glaucoma Society Annual Meeting, Washington, DC, United States, February 27–March 2, 2014.

Supported in part by National Eye Institute Vision Core Grant P30EY010608, a Challenge Grant from Research to Prevent Blindness to The University of Texas Medical School at Houston, and the Hermann Eye Fund. The CASIA SS-1000 was loaned by the Tomey Corporation (RMF).

Disclosure: **L.S. Blieden**, None; **A.Z. Chuang**, None; **L.A. Baker**, None; **N.P. Bell**, None; **T.S. Fuller**, None; **K.A. Mankiewicz**, None; **R.M. Feldman**, Tomey Corporation (F)

References

1. Quigley HA, Silver DM, Friedman DS, et al. Iris cross-sectional area decreases with pupil dilation and its dynamic behavior is a risk factor in angle closure. *J Glaucoma*. 2009;18:173–179.
2. Quigley HA. Angle-closure glaucoma—simpler answers to complex mechanisms: LXVI Edward Jackson Memorial Lecture. *Am J Ophthalmol*. 2009;148:657–669.
3. Aptel F, Denis P. Optical coherence tomography quantitative analysis of iris volume changes after pharmacologic mydriasis. *Ophthalmology*. 2010;117:3–10.
4. Leung CK, Weinreb RN. Anterior chamber angle imaging with optical coherence tomography. *Eye (Lond)*. 2011;25:261–267.
5. Console JW, Sakata LM, Aung T, Friedman DS, He M. Quantitative analysis of anterior segment optical coherence tomography images: the Zhongshan Angle Assessment Program. *Br J Ophthalmol*. 2008;92:1612–1616.
6. Kim DY, Sung KR, Kang SY, et al. Characteristics and reproducibility of anterior chamber angle assessment by anterior-segment optical coherence tomography. *Acta Ophthalmol*. 2011;89:435–441.
7. Liu S, Yu M, Ye C, Lam DS, Leung CK. Anterior chamber angle imaging with swept-source optical coherence tomography: an investigation on variability of angle measurement. *Invest Ophthalmol Vis Sci*. 2011;52:8598–8603.
8. Radhakrishnan S, See J, Smith SD, et al. Reproducibility of anterior chamber angle measurements obtained with anterior segment optical coherence tomography. *Invest Ophthalmol Vis Sci*. 2007;48:3683–3688.
9. Liu S, Li H, Dorairaj S, et al. Assessment of scleral spur visibility with anterior segment optical coherence tomography. *J Glaucoma*. 2010;19:132–135.
10. Sakata LM, Lavanya R, Friedman DS, et al. Assessment of the scleral spur in anterior segment optical coherence tomography images. *Arch Ophthalmol*. 2008;126:181–185.
11. Rigi M, Blieden LS, Nguyen D, et al. Trabecular-iris circumference volume in open angle eyes using swept-source Fourier domain anterior segment optical coherence tomography. *J Ophthalmol*. 2014;2014:590978.
12. Foster PJ, Buhrmann R, Quigley HA, Johnson GJ. The definition and classification of glaucoma in prevalence surveys. *Br J Ophthalmol*. 2002;86:238–242.
13. Spaeth GL. The normal development of the human anterior chamber angle: a new system of descriptive grading. *Trans Ophthalmol Soc U K*. 1971;91:709–739.
14. Spaeth GL, Aruajo S, Azuara A. Comparison of the configuration of the human anterior chamber angle, as determined by the Spaeth gonioscopic grading system and ultrasound biomicroscopy. *Trans Am Ophthalmol Soc*. 1995;93:337–347, discussion 347–351.
15. Cumba RJ, Radhakrishnan S, Bell NP, et al. Reproducibility of scleral spur identification and angle measurements using Fourier domain anterior segment optical coherence tomography. *J Ophthalmol*. 2012;2012:487309.

16. Pavlin CJ, Harasiewicz K, Foster FS. Ultrasound biomicroscopy of anterior segment structures in normal and glaucomatous eyes. *Am J Ophthalmol*. 1992;113:381–389.
17. Radhakrishnan S, Goldsmith J, Huang D, et al. Comparison of optical coherence tomography and ultrasound biomicroscopy for detection of narrow anterior chamber angles. *Arch Ophthalmol*. 2005;123:1053–1059.
18. Memarzadeh F, Li Y, Chopra V, Varma R, Francis BA, Huang D. Anterior segment optical coherence tomography for imaging the anterior chamber after laser peripheral iridotomy. *Am J Ophthalmol*. 2007;143:877–879.
19. Lee KS, Sung KR, Shon K, Sun JH, Lee JR. Longitudinal changes in anterior segment parameters after laser peripheral iridotomy assessed by anterior segment optical coherence tomography. *Invest Ophthalmol Vis Sci*. 2013;54:3166–3170.
20. Aptel F, Beccat S, Fortoul V, Denis P. Biometric analysis of pigment dispersion syndrome using anterior segment optical coherence tomography. *Ophthalmology*. 2011;118:1563–1570.
21. Nguyen D, Bell NP, Blieden LS, Baker LA, Chuang AZ, Feldman RM. Effect of laser peripheral iridotomy on trabecular-irido circumference volume in primary angle closure eyes. Poster presented at: American Glaucoma Society 23rd Annual Meeting; February 28–March 2, 2013; San Francisco, CA.
22. Zhang Y, Li SZ, Li L, He MG, Thomas R, Wang NL. Quantitative analysis of iris changes after physiologic and pharmacologic mydriasis in a rural Chinese population. *Invest Ophthalmol Vis Sci*. 2014;55:4405–4412.
23. Aptel F, Chiquet C, Beccat S, Denis P. Biometric evaluation of anterior chamber changes after physiologic pupil dilation using Pentacam and anterior segment optical coherence tomography. *Invest Ophthalmol Vis Sci*. 2012;53:4005–4010.
24. Narayanaswamy A, Zheng C, Perera SA, et al. Variations in iris volume with physiologic mydriasis in subtypes of primary angle closure glaucoma. *Invest Ophthalmol Vis Sci*. 2013;54:708–713.
25. Tun TA, Baskaran M, Perera SA, et al. Sectoral variations of iridocorneal angle width and iris volume in Chinese Singaporeans: a swept-source optical coherence tomography study. *Graefes Arch Clin Exp Ophthalmol*. 2014;252:1127–1132.
26. Mak H, Xu G, Leung CK. Imaging the iris with swept-source optical coherence tomography: relationship between iris volume and primary angle closure. *Ophthalmology*. 2013;120:2517–2524.
27. See JL. Imaging of the anterior segment in glaucoma. *Clin Experiment Ophthalmol*. 2009;37:506–513.
28. Salzmann M. The iris. In: Brown EVL, trans. *The Anatomy and Histology of the Human Eyeball in the Normal State: Its Development and Senescence*. Chicago: The University of Chicago Press; 1912:125–148.

Investigative Ophthalmology & Visual Science